Discriminant Analysis with Spatial Weights for Urban Land Cover Classification

Wentz, E.A. Song, Y. Anderson, S.
Roy, S.S. Myint, S.W. Stefanov, W.L

2010

Working Paper Number 21

Discriminant analysis with spatial weights for urban land cover classification

ELIZABETH A. WENTZ[†*]
YANG SONG[†]
SHAROLYN ANDERSON[‡]
SHOURSASENI SEN ROY [§]
SOE W. MYINT[†]
WILLIAM L. STEFANOV[¶]

[†]School of Geographical Sciences
Arizona State University
Tempe, AZ 85287-0104
wentz@asu.edu
480-965-3315 (voice)
480-965-8313 (fax)

[‡]Department of Geography
University of Denver
Denver, CO 80208

[§] Department of Geography and Regional Studies
University of Miami
Coral Gables, Florida 33124

[¶]Image Science & Analysis Laboratory/ESCG
NASA Johnson Space Center
Houston, TX 77058 USA

*corresponding author. Email address: wentz@asu.edu

Discriminant analysis with spatial weights for urban land cover classification

Abstract
Classifying urban area images is challenging because of the heterogeneous nature of the urban landscape resulting in mixed pixels and classes with highly variable spectral ranges. Approaches using ancillary data, such as knowledge based or expert systems, have shown to improve the classification accuracy in urban areas. Appropriate ancillary data, however, may not always be available. The goal of this study is to compare the results of the discriminant analysis statistical technique with discriminant analysis with spatial weights to classify urban land cover. Discriminant analysis is a statistical technique used to predict group membership for a target based on the linear combination of independent variables. Strict per pixel statistical analysis however does not consider the spatial dependencies among neighbouring pixels. Our study shows that approaches using ancillary data continue to outperform strict spectral classifiers but that using a spatial weight improved the results. Furthermore, results show that when the discriminant analysis technique works well then the spatially weighted approach performs better. However, when the discriminant analysis performs poorly, those poor results are magnified in the spatially weighted approach in the same study area. The study shows that for dominant classes, adding spatial weights improves the classification accuracy.

1. Introduction

Remotely sensed data provide abundant information for urban area analyses because of the extensive spatial and temporal coverage and the broad spectral range of the data. Researchers have been using remotely sensed data in urban areas for numerous applications such as characterizing and monitoring urban sprawl at various spatial scales (Jat et al. 2008; Wentz et al. 2006; Keys et al. 2007; Stefanov and Netzband 2005, 2010; Ji et al. 2001), mapping impervious surfaces (Weng and Lu 2008), monitoring building construction (Durieux et al. 2008), extracting urban tree locations (Ouma and Tateishi 2008), estimating population (Welch 1980), calculating temperature of urban surfaces (Chen et al. 2005), estimating the extent and intensity of the urban heat island effect (Weng et al. 2004; Lo et al. 1997; Sutton et al. 2009), and assessing urban air quality (Sohrabinia and Khorshiddoust 2007; Silvia et al. 2006). The importance and impact of these data for understanding the drivers and consequences of urban expansion will continue to grow (Longley 2002; Sutton et al. 2006).

A common task in urban remote sensing analysis is the identification and classification of land cover – the distribution of physical materials comprising the land surface within a given area, with subsequent transformation into land use – the human activity associated with that given area (Barnsley et al. 2001). Land cover classification involves developing an algorithm to analyze the spectral range of pixels and organize them into meaningful descriptions of the land surface. The land cover categories can then be refined into user-defined categories of human use. One of the difficulties in accurately identifying urban land use is the highly heterogeneous nature of land covers within a single land use (Myint et al. 2007). For example, a residential land use will be spatially and spectrally complex because of the combination of variable roof types, heterogeneous landscaping, asphalt, and other small features. These land covers combined constitute one land use type. The diversity of urban land cover types and the mixture of covers within a

given land use lead to two possible phenomena in remote sensing image classification: mixed pixels and the speckle effect.

The concept of a 'mixed' pixel refers to a single pixel value that is the combination of multiple reflectance or emissivity values recorded by the remote sensor at a given location. The ideal 'pure' pixel would record only one type of ground reflectance or emissivity. While the effect is reduced when the pixel size is quite small (e.g., less than 1 meter), an urban area image with only pure pixels does not exist. To compensate, the general goal is to deconvolve or "unmix" the pixel spectral signature into its dominant components. Common techniques used to reduce the data dimension include principle component analysis (Cortijo and Blanca 1999), multiple endmember spectral mixture analysis (Rashed et al. 2003; Powell et al. 2007), and adaptive mean shift analysis (Huang and Zhang 2008). The resulting classified image, however, will have an expected amount of error and uncertainty.

In addition to the mixed pixel problem, the speckle effect refers to isolated individual pixels that are classified differently than a majority of the surrounding pixels. This phenomenon is particularly evident when using Synthetic Aperture Radar (SAR) data and dealing with data collection noise (Hebar et al. 2009). In an urban context, the cause of speckle effect is simply misclassification of individual pixels as a result of the heterogeneous nature of the landscape. This is because traditional classifiers focus only on the statistical separation of classes for individual pixels and ignore neighborhood relationships. For example, there may be a rocky outcrop in an undeveloped area near a city covering an area of one pixel. This pixel may be classified into a 'concrete' category because of the spectral similarity between rocks and road surfaces, even though the surrounding pixels are undeveloped. To minimize the speckle effect, researchers have tested spatial filters, kernel-based approaches, neural networks and object-oriented approaches. Spatial filters and kernel-based approaches use strict neighborhood relationships to reassign values, acting as a smoothing function (Alimohammadi and Shirkavand 2010). Object-oriented methods organize neighbouring pixels with similar spectral information into objects prior to classification (Burnett and Blaschke 2003; Forester et al. 2009; Platt and Rapoza 2008; Foody 2003). These methods have improved the speckle effect, particularly with high-resolution imagery, but the challenge is determining the best kernel or object size for a particular application without loss of information.

Another major advancement in urban remote sensing image classification is the development of expert system approaches (also known as knowledge-based algorithms). Expert system approaches apply decision rules and ancillary data along with spectral information to classify a pixel (Stefanov et al. 2001; Stefanov and Netzband 2005, 2010; Su et al. 2010; Wentz et al. 2008). Ancillary data (e.g., elevation, zoning classification, road networks) provide contextual information by defining the boundaries and adding information that can be used in both classification and in post-classification recoding of results (Stefanov et al. 2001). These methods represent a clear advancement to spectral-only pixel classifiers because the resulting classified image has more refined classes (usually more classes, particularly in urban areas) and a higher overall accuracy. The disadvantages are that classification rules need to be customized for each image or study area and the needed ancillary data are not always available (Wentz et al. 2008). There

remains a need, therefore, for methods that depend less on ancillary data and focus only on spectral information and neighbourhood relationships.

The objective of this study is to adapt the discriminant analysis statistical technique, which is used in remote sensing image classification (Qian and Nekovei 2005), to include spatial weights to classify urban land cover. The discriminant analysis with spatial weights (DASW) approach has the same advantages of pixel-based classifiers, but also addresses the problem of spatial complexity of the urban land surface to deal with the speckle effect. This approach is not a smoothing method as other kernel methods are because pixel assignment requires that both neighborhood and spectral requirements are met. Our hypothesis is that by adding a spatial weight to each pixel, the final urban land cover classification result will reflect local similarity of land cover types for pixels that have slightly different spectral values. Our approach is tested empirically on classifying urban land cover in Phoenix Arizona.

2. Methods

2.1 Study area

The Phoenix metropolitan area was selected as a case study for this research because of the rapid growth has led to considerable land cover analysis research using remotely sensed data. In 2007, the US Census estimated that from April 2000 to July 2006 the Phoenix area grew at a rate of 24.2%, which places the area among the top 5 metropolitan areas for population growth (US Census 2007). By comparison, the average urban area grew by only 6.2% (US Census 2007). The results of population growth on the landscape are a quantifiable change from predominantly agriculture to low and medium density residential (Keys et al. 2007). The pattern of land use is more diverse from the original simple open desert/agriculture into mixed residential, commercial and industrial areas. To reflect the diversity of the urban landscape and to reduce computational time needed to test and evaluate the techniques, we selected three 900 km^2 regions within the Phoenix Arizona metropolitan area. The three regions include an urban fringe area (Figure 1b), an urban core area (Figure 1c), and a residential/agricultural area (Figure 1d), representing the variation in possible land covers for the area.

2.2 Data

Data used in this study are Advanced Spaceborne Thermal Emission and Reflection Radiometer (ASTER) images and aerial photographs. ASTER images are high spatial resolution data (15 m/pixel) in the visible/near-infrared wavelengths and have been used in urban land use/land cover research studies (Stefanov and Netzband 2005, 2010; Shobeiri et al. 2007). We selected two level-2 ASTER images from September 19, 2000 as the source data for classification. These two images contain atmospherically corrected surface reflectance data in the visible and near-infrared bands. The image quality is clear with cloud cover below 5%. Both images were projected into Universal Transverse Mercator (UTM) Zone 12 coordinate system and mosaicked together. The spatial coverage for the ASTER images contains northeast Phoenix, the Salt River, and the nearby, undeveloped desert. The three study areas were extracted from this image. Each region has one million pixels (1000 by 1000) with 15-meter resolution per pixel (Figure 1a).

An aerial photo of the study area was used as reference for the accuracy assessment. The aerial photo was acquired in 1999 from the Central Arizona-Phoenix Long Term Ecological Research (CAP LTER) Project at Arizona State University. The projection is the same as the ASTER images (UTM zone 12 projection, WGS 84 datum). The pixel size is 3 x 3 meters.

2.3 Image classification

The ASTER data were classified with Discriminant Analysis (DA) and Discriminant Analysis with Spatial Weights (DASW). We used 578 points as the training set for the DA, the same as those from Stefanov and Netzband (2005). There are 11 classes: asphalt, soil/bedrock, fluvial sediments, water, agricultural vegetation, agricultural soil, undifferentiated vegetation, grass/shrub, mesic residential, xeric residential, and reflective built surfaces. The distinction between xeric and mesic residential is that the xeric landscaping tends to be low or non-irrigated, which typically results in a lower amount of vegetation cover. The average number of points for each class is 52 with a standard deviation of 14.71.

DA is a statistical technique used to predict group membership for a target based on the linear combination of independent variables. Like other statistical classification algorithms, DA is based purely on the intrinsic statistical characteristics of the source data. There are no spatial parameters involved during the classification process. For example, a DA would classify a pixel into 'asphalt' providing the spectral values satisfy the mathematical equation for that land cover type. The classification results are not adjusted based on neighbouring values. However our expectation is that if that pixel is near or inside a residential area, it may have a higher probability of being a residential land use. The algorithm for linear discriminant analysis (LDA) is based on Bayes theory. For a given population with i classes, calculate the posterior probability for each class and select the one with the highest value as the final classification result, i.e.

$k = \max (p_i f_i(\mathrm{x}))$, where k is the classified group, p_i is the prior probability, $f_i(x)$ is the probability density function (likelihood).

For a supervised remote sensing classification, the training sets are selected to calculate the prior probability p and likelihood $f(x)$. In this study, we used the 578 random points throughout the study area and identified them into the same 11 land cover classes as the expert system classification results reported by Stefanov and Netzband (2005). The posterior probability k for each class is then calculated with SPSS software. For a given pixel, the highest posterior probability among 11 classes is the final classification result of discriminant analysis.

Brunsdon et al. (2007) developed Geographical Weighted Discriminant Analysis (GWDA) based on the frameworks of geographically weighted regression (GWR) and discriminant analysis. GWDA replaces the global variables in DA with localized variables with spatial information. The main purpose of GWDA is to highlight the local heterogeneity, which is usually hidden in a global classification, by implementing a geographical weight to the linear combination of variables:

$k = \max (W_i p_i f_i(\mathrm{x}))$, where k is the classified group, p_i is the prior probability, $f_i(x)$ is the probability density function (likelihood), W_i is the geographical weight.

We used the inversed distance weighted (IDW) density to calculate the W_i. First, we applied an n by n window to the source data image. The spatial distance D_i between a pixel (x_i, y_i) and the centre pixel of the window (x, y) is calculated as:

$$D_i = \sqrt{(x_i-x)^2+(y_i-y)^2}$$

The inversed distance weight is:

$$IDW = 1/ D_i = 1 / \sqrt{(x_i-x)^2+(y_i-y)^2}$$

The density D_i is calculated as:

$D_i = n_i/n$, where n_i is the number of pixels for class i, n is the total number of pixels inside the window.

The final geographical weight W_i is calculated as:

$$W_i = IDW * D_i = 1 / \sqrt{(x_i-x)^2+(y_i-y)^2} * n_i/n$$

This inversed distance weight emphasizes both spatial distance and density. The general assumption is that for a given window size (n x n), the neighbouring pixels will have influence on the centre pixel based on their relative distance and the density.

The GWDA application in Brunsdon et al. (2007) was based on the election voting results of the United Kingdom in 2005 with geographic data in vector format. Brunsdon et al. (2007) proposed the nearest neighbour algorithm and cross-validation to calculate the kernel bandwidth. Although our approach is inspired by GWDA, we call the approach used here discriminant analysis with spatial weights (DASW) to distinguish it from GWDA because we did not use their software and our approach uses raster data and window size as the bandwidth.

Due to the issue of spatial variability in the landscape, the fixed bandwidth may not always be the best choice. For example, in the fringe section of our study (Figure 2b), it is reasonable to expect that there will be less spatial variety in relatively homogeneous land surfaces (such as desert/bare soil) and high spatial variety in relatively heterogeneous land surfaces (such as residential areas). Therefore a fixed kernel bandwidth (3 by 3 window size) may not be suitable for all the classes. An adaptive window size is necessary for distinguishing the spatial variety among different scales.

In Brunsdon et al. (2007), the adaptive bandwidth was implemented by the nearest neighbour algorithm using a vector source data. The geographical distance of the designated nearest neighbour to the centre data unit was considered the adaptive bandwidth. In this study with raster remote sensing images, we used the kernel function 'diversity' to calculate the adaptive window size. For each pixel, the window size increases from 3 by 3 to 5 by 5, 7 by 7, 9 by 9…until the number of classes inside the window is equal or larger than 6 (which represent at least half of the total 11 classes).

2.4 Accuracy assessment

We generated 110 points to validate the classification results based on the land cover data and aerial photos. The n-size (n=110) was selected based on the number of categories (11 total) and a minimum of 10 points per category. The assessment was calculated for each approach, discriminant analysis (DA) and discriminant analysis with spatial weights using a fixed bandwidth (DASW_F), discriminant analysis with an adaptive bandwidth (DASW_A), and the Stefanov and Netzband (2005) expert system (ES). These approaches were compared using a confusion matrix, user / producer accuracy and overall accuracy. We recalculated the ES accuracies for each of the three individual areas

in this study, resulting in accuracy values different from those reported in Stefanov and Netzband (2005).

3. Results

The overall accuracy for the four approaches for the three st udy areas is reported in Table 1. Consistently, the ES outperformed the three DA approaches with the DA without spatial weights typically performing the worst. In this section, we describe the results for the individual study areas.

3.1 Urban core

The urban core section of the study area contains the Salt River and Tempe Town Lake, Sky Harbor airport, two mountain areas and residential and commercial buildings (Figure 2). The overall classification accuracies for the different techniques were 16.5% (DA), 33.6% (DASW_F), 31.8% (DASW_A), and 66.3% (ES). Although the ES approach performed the best, these are all below the desired 85% level. The agriculture and vegetation categories consistently had the highest accuracy regardless of the classification approach used. This is due to the homogeneity of the class type. The weakest categories were the residential categories (Table 2).

The DA approach resulted in no dominant classes, which is defined here as greater than 25% of the study area represented by a single class (Table 3). The class with the highest percent was soil/bedrock at 13.4%. The user and producer accuracy, however, were low (15.4% and 9.1% respectively), suggesting little confidence that this is reflective of the area. Little improvement was made using the spatially weighted approaches. The weighting increased the percentage of the agriculture soil class to nearly 20% using the DASW_A. The biggest shift happened however, with the xeric residential class, which increased from 6.4% (DA) to 39.6% (DASW_F) and 39.9% (DASW_A). The user and producer accuracies for xeric residential using these techniques showed an improvement (76.9% and 41.7% for DASW_F and 69.2% and 40.9% for DASW_A).

For the ES approach, which had the highest overall accuracy and the best user and producer statistics, most of the pixels were classified into soil/bedrock (37.8%) and xeric residential (23.9%), which reflects the dominating classes expected in the urban core. The soil/bedrock and xeric residential is similar to the DA approach as well. The user and producer accuracy were 38.9% and 70.0% for the soil/bedrock and 44.4% and 80.0% for the xeric residential. All of the accuracy scores are higher than the DA approaches. Classes with lowest area percentage were water (0.5%) and undifferentiated vegetation (0.6%).

3.2 Residential/Agricultural

The expected dominant classes in the residential/agricultural study area are xeric and mesic residential followed by agricultural soil/vegetation (located mostly in the southeastern section of the area; Figure 3). Like the urban core section, the ES performed the best with an overall accuracy score of 60.0% followed by the DASW_A at 29.1% (Table 4). The weakest was the DA without spatial weights with an overall accuracy score of 19.1%. The classes with the highest accuracy scores were fluvial sediment, agricultural vegetation, and grass/shrubs, although they are not the classes that dominate the area.

According to the ES approach, the area is dominated by soil/bedrock (34.5%) followed by xeric residential (21.9%), (Table 5). The agriculture categories (soil and vegetation) together represent close to 15% of the study area with high user and producer accuracy scores (100%). The high accuracy is because of the uniform characteristics of the landscape.

The DA approach was ineffective at classifying this area with an overall score of 19.1%. DA consistently misclassified asphalt as water, which was corrected in the spatially weighted DA. The spatially weighted DA approaches (DASW_F and DASW_A) had xeric residential followed by agriculture soil/vegetation as the dominant classes, which is what was expected. The user and producer accuracy scores, however, for these classes were below 50% in all cases.

3.3 Urban fringe

The results for the urban fringe area were consistent with the other two areas with accuracy scores highest for the ES approach (58.1%), (Figure 4, Table 6). In this case, however, the DA without spatial weights outperformed the DASW_A approach with overall accuracy scores at 20.9% and 15.4% respectively. The DASW_F, however, was a slight improvement (at 21.8%) over the DA. This suggests that in an area with considerable heterogeneity, like the urban fringe, adding *adaptive* spatial weights reduced the overall accuracy score. Theoretically speaking, the urban fringe is heterogeneous and the adaptive bandwidth should be more suitable for these situations. Our results do not support this theory.

The dominant classes in this area are xeric residential (represented by newer construction, typical of the urban fringe), and soil/bedrock (typical of undeveloped deserts and mountains), (Table 2). The ES approach reports 51.8% of the area is soil/bedrock followed by 23.9% being xeric residential. The user and producer accuracy scores were high for both classes. The xeric residential had user and producer accuracy scores of 62.5% and 90.9% and the soil/bedrock scores were 60.0% and 90.0%.

Like the residential study area, the DA incorrectly classified numerous bedrock pixels as water. The spatially weighted DA approaches changed these and classified them into either bedrock (correct classification) or asphalt (incorrect classification). The DA approaches also were unable to effectively identify the xeric residential areas as well as the ES approach in the urban fringe.

3.4 Speckle comparison

One of the expectations was that adding fixed or adaptive spatial weights to the DA would reduce the speckles visible in the resulting image. The approach to evaluate this is to compare the change of area percentage for the dominating classes (mesic/xeric residential combined) and minor classes (asphalt, water, fluvial sediments, grass/shrub, undifferentiated vegetation, and reflective surfaces). The dominant class for the fringe area would also include soil/bedrock according to ES classification result. We compared both of the non-weighted approaches (ES and DA) to the spatially weighted approaches (DASW_F and DASW_A).

For the urban core study area, the DASW_F approach increased the dominating class of mesic and xeric residential. Likewise, the accuracy for these classes improved as compared to the DA approach. The area percentage combined together (56.8%) is

approximately 177% larger than the ES (32.0%) and 288% larger than DA (19.7%). The minor classes combined together reduced to 14.5%, approximately 53% of the ES (27.6%) and 26% of DA (56.2%). DASW_A further reduced the minor classes combined together to 11.1%, approximately 40% of ES and 20% of DA. The dominating mesic/xeric class for DASW_A combined together (58.86%) is approximately 183% larger than ES and 298% larger than DA.

In the residential/agricultural study area, the DASW_F were 111% larger than ES and 234% larger than DA for the combined mesic/xeric residential classes. The area of the minor classes for DASW_F was slightly larger compared to ES, but was still smaller compared to DA. DASW_A further increased the dominating classes to120% larger than ES and 251% larger than DA. The minor classes in DASW_A were also reduced.

For the urban fringe study area of Phoenix, the dominating classes in DASW_F were 49% less than the ES and 88% less than DA. The area for minor classes in DASW_F was 162% larger than the ES approach and 60% less than DA. DASW_A had only 39% of the ES and 69% of DA. The minor classes for DASW_A are 128% larger than ES and 47% of DA.

4. Discussion

Our significant finding was that when the DA worked well, adding the spatial weights worked better. However, we also learned that when DA did not perform well, adding the spatial weights magnified those problems in the same area. This is because the algorithm is designed to reduce the area of minor classes and increase the area of dominating classes. For example, in the urban core, the overall accuracy nearly doubled (from nearly 16% to over 33%) when adding the spatial weights. The accuracy scores for individual classes, such as mesic residential in the urban fringe area, are low for the DA (9.5%) and are lower for the spatially weighted approaches (4.8%). In another example, when the DA approach worked reasonably well (e.g., soil/bedrock in the urban fringe area), the spatial weights were an improvement (with an increase in producer accuracy from 40% to 80%). This suggests that the spatial weights approach depends significantly on the accuracy of the underlying classification approach. The original intent of the spatial weights was to improve the DA accuracy but the reliance on the accuracy of the DA hinders independent improvement. This leads to a specific question on the quantitative threshold for the DASW application to improve DA.

The specific results obtained in the urban fringe area illustrate this further. Our classification results using DA were very poor in this area. Most of the asphalt pixels were misclassified into water and there was a large amount of soil/bedrock pixels misclassified into vegetation in the north mountain. Due to the heterogeneous land covers in this area, there were heavy ‘speckles’ in the DA classification result. When the spatial weights were added to the DA, the DASW almost eliminated all the minor classes. Table 2 shows there are more ‘N/A’ in the urban fringe study area (section c) compared to the other two study areas (Table 2, sections a and b). DASW with adaptive bandwidth outperformed DASW with fixed bandwidth using a visual inspection, which shows that DASW_F is still a little bit more “speckled” than DASW_A. So in the case of the speckle effect, DASW_A did outperform DASW_F. Nevertheless, with respect to class accuracy (Table 2), DASW_A does not outperform DASW_F. This represents the ’magnifying

effect' on the underlying classification error mentioned previously. With respect to class accuracy, the DA results are poor, DASW is worse, and DASW_A has worse accuracy than DASW_F.

By design, the spatial weights had the result of increasing the area of the dominant classes and decreasing the area of the minor classes. We can view this as an improvement since the resulting accuracy scores for these classes also improved. The most significant improvement occurs from the DA to the DASW with either a fixed or adaptive bandwidth. Little or no improvement existed between the ES and the spatially weighted approaches. The adaptive bandwidth outperformed the fixed bandwidth in the urban core and the urban fringe areas, where there were larger regions of homogeneous land cover types, such as soil/bedrock.

Our findings have led us to propose more specific distinctions for 'homogeneous' and 'heterogeneous' landscapes. We need to qualify each with both 'locally' and 'globally.' The urban fringe region has a mountainous area in the north that covers a large portion of the study area. These large areas of the same type of land cover (e.g., a mountain area) are locally homogeneous because neighbouring pixels have similar spectral values. In contrast, a large area of residential is locally heterogeneous because of the variability of the land covers, which would include a mixture of vegetation, asphalt, and rooftop composition. Nevertheless, both the locally homogenous mountains and the locally heterogeneous residential land cover co-exist in the same urban fringe section. As a study area, this area can then be described as 'globally heterogeneous.' This further distinguishes the DASW approach from GWDA because the spatial weights in our application are calculated locally rather than globally.

One of the problems resulting from DASW is that a visual inspection of our results shows class boundaries as rounded and distorted from what might be expected. The Phoenix area urban landscape has crisp boundaries with many right angles. Agriculture, followed by streets and the subsequent residential subdivisions, follow a rectangular grid pattern. The DASW approaches rounded these boundaries. Nearly all of the roads were distorted to some extent in DASW. The boundaries of agricultural vegetation also became irregular as well. This is because the DASW algorithm is based on an *n by n* window, equally spaced from a central pixel. The calculation of geographical weight is derived from the inversed distance and density inside the window. This distortion effect is more apparent with the adaptive bandwidth, as illustrated in the figures. The shape preservation is not specifically designed into the algorithm. To solve this distortion effect, two possible suggestions are to reduce the window size for specific classes or to set the non-boundary classes to zero when the window is moving on a boundary. This distortion phenomenon suggested that DASW may be a less suitable approach when high boundary precision is required. To resolve this, an analyst could extract the edge information from ancillary data so that the window size or geographical weight could be set to zero for all the non-boundary classes. This will ensure the shape of the original boundary is not distorted by the DASW classification.

While the primary objective in this research was to develop a method that could classify urban land cover effectively using multispectral remotely sensed information without ancillary data, a clear method to improve overall accuracy would be to add a spatial weight to an approach such as ES that uses ancillary data. With ancillary data, such as roads, elevation, or zoning boundaries, decision rules can be established that help

distinguish between classes with similar spectral signatures. Using an object-oriented approach (OBIA), as demonstrated by Su et al. (2010), a spatial weight could improve the accuracy results and reduce the speckle effect, as illustrated here with DA. As already stated, the ancillary data could be used to refine the boundaries that become distorted with the weighting factor.

5. Conclusions

This study illustrated that under specific conditions, fixed and adaptive bandwidth DASW can be an effective method to classify urban land cover and reduce the speckle effect. In certain cases, DASW also improves the classification accuracy over DA alone. The improvements were most significant in areas that are more homogeneous, such as agriculture and bedrock areas. While we would have liked to see improved results in the heterogeneous areas as well, these areas continue to be a challenge without ancillary data.

Classification of urban land cover remains a significant challenge. Higher resolution data and better spectral ranges improve the results but new challenges emerge. The new challenge in urban remote sensing classification is the improvement of signal/noise ratio of the output map. Remote sensing images with high spatial and spectral resolution have provided abundant useful information as well as a large amount of noise. A small fraction of water can be identified inside large areas with buildings with an accurate statistical classification method. The classification result for the swimming pool is statistically correct, however, this type of information would be considered as a noise for a city planner working on a larger geographic scale. While techniques such as DASW improve this, we still need methods to efficiently reduce the speckle effect and increase the signal/noise ratio for the output map.

Future studies on using spatial DASW application in remote sensing classification should focus on the identification of dominating and minor classes. The evaluation of DA accuracy is one important procedure before DASW classification. This requires additional ground truth data to validate the DA classification results. Furthermore, there should also be a quantifiable threshold below which the DASW is not considered an improvement to the DA.

References

Alimohammadi, A and Shirkavand, M, 2010, Adaptive spatial reclassification kernels for urban mapping from remotely sensed data: the A-SPARK approach, International Journal of Remote Sensing 31(3): 761-774.

BARNSLEY, M.J., MØLLER-JENSEN, L., BARR, S.L., 2001, Inferring urban land use by spatial and structural pattern recognition, in DONNAY, J-P, BARNSLEY, M.J., AND LONGLEY, P.A., eds., *Remote Sensing and Urban Analysis,* Taylor & Francis, London, pp. 116-144.

BRUNSDON, C, FOTHERINGHAM, S, and CHARLTON, M., 2007, Geographical weighted discriminant analysis *Geographical Analysis* **39** pp. 376-396.

BURNETT, C., and BLASCHKE, T., 2003, A multi-scale segmentation/object relationship modelling methodology for landscape analysis *Ecological Modelling* **168 (3)** pp. 233-249.

CHEN, X., VIERLING, L. and DEERING, D., 2005, A simple and effective radiometric correction method to improve landscape change detection across sensors and across time *Remote Sensing of Environment* **98** pp. 63-79.

CORTIJO, F., and BLANCA, N., 1999, The performance of regularized discriminant analysis versus non-parametric classifiers applied to high-dimensional image classification *International Journal of Remote Sensing* 20 **pp**. 3345-3365.

DURIEUX, L., LAGABRIELLE, E. and NELSON, A., 2008, A method for monitoring building construction in urban sprawl areas using object-based analysis of Spot 5 images and existing GIS data. *ISPRS Journal of Photogrammetry and Remote Sensing*, **63** pp. 399-408.

FOODY, G., 2003, Geographical weighting as a further refinement to regression modeling: An example focused on the NDVI–rainfall relationship. *Remote Sensing of Environment* **88** pp. 283–293.

FORSTER, D., BUEHLER, Y., and KELLENBERGER, T. W. 2009, Mapping urban and peri-urban agriculture using high spatial resolution satellite data *Journal of Applied Remote Sensing* **3** Article Number: **033523**.

HEBAR, M., GLEICH, D., and CUCCJ, Z., 2009, Autobinomial Model for SAR Image Despeckling and Information Extraction *IEEE Transactions on Geoscience and Remote Sensing* **47** pp. 2818-2835**.**

HUANG, X., ZHANG, L., 2008, An adaptive mean-shift analysis approach for object extraction and classification from urban hyperspectral imagery. *Geoscience and Remote Sensing* **46** pp. 4173-4185.

JAT, M. K., GARG, P. K., and KHARE, D., 2008, Monitoring and modelling of urban sprawl using remote sensing and GIS techniques *International Journal of Applied Earth Observation and Geoinformation* **10** pp. 26-43.

JI, C. Y., LIU, Q., SUN, D., WANG, S., LIN, P. and LI, X., 2001, Monitoring urban expansion with remote sensing in China *Remote Sensing of Environment* **22** pp. 1441-1455.

KEYS, E., WENTZ, E. A., and REDMAN, C. L., 2007, The spatial structure of land use from 1970-2000 in the Phoenix, Arizona, metropolitan area *The Professional Geographer* **59** pp. 131-147.

LO, C. P., QUATTROCHI, D. A. and LUVALL, J. C., 1997, Application of high-resolution thermal infrared remote sensing and GIS to assess the urban heat island effect *Remote Sensing of Environment* **18** pp. 287-304.

LONGLEY, P. A., 2002, Geographical Information Systems: will developments in urban remote sensing and GIS lead to 'better' urban geography? *Remote Sensing of Environment* **26** pp. 231-239.

MYINT, S. W., WENTZ, E. A., and PURKIS, S. J., 2007, Employing spatial metrics in urban land-use/land-cover mapping: Comparing the Getis and Geary indices *Photogrammetric Engineering and Remote Sensing* **73** pp. 1403-1415**.**

OUMA, Y. O., and TATEISHI, R., 2008, Urban-trees extraction from Quickbird imagery using multiscale spectex-filtering and non-parametric classification *ISPRS Journal of Photogrammetry and Remote Sensing* **63** pp. 333-351.

PLATT, R., and RAPOZA, L., 2008, An evaluation of an object-oriented paradigm for land use/land cover classification *The Professional Geographer* **60** pp. 87-100.

POWELL, R., ROBERTS, D., and DENNISON, P., 2007, Sub-pixel mapping of urban land cover using multiple endmember spectral mixture analysis: Manaus, Brazil. *Remote Sensing of Environment* **106** pp. 253–267.

QIAN, D., and NEKOVEI, R., 2005, Implementation of real-time constrained linear discriminant analysis to remote sensing image classification. *Pattern Recognition* **38** pp. 459 -471.

RASHED T., WEEKS J. R., ROBERTS D., ROGAN J., POWELL R., RIO, J., and LOZANO-GARCIA, D., 2003, Measuring the physical composition of urban morphology using multiple endmember spectral mixture models *Photogrammetric engineering and remote sensing,* **69** pp. 1011-1020.

SHOBEIRI, S. M., OMIDVAR, B. and PRAHALLAD A., 2007, Digital change detection using remotely sensed data for monitoring green space destruction in Tabriz *International Journal of Environmental Research* **1** pp. 35-41.

SILVIA, F., ILARIA, C., and STEFANIA, M., 2006, Integrating remote sensing approach with pollution monitoring tools for aquatic ecosystem risk assessment and management: a case study of Lake Victoria (Uganda) *Environmental Monitoring and Assessment* **122** pp. 275-287.

SOHRABINIA, M., and KHORSHIDDOUST, A. M., 2007, Application of satellite data and GIS in studying air pollutants in Tehran *Habitat International* **31** pp. 268-275.

STEFANOV, W. L., RAMSEY, M. S., and CHRISTENSEN, P. R., 2001, Monitoring urban land cover change: an expert system approach to land cover classification of semiarid to arid urban centers *Remote Sensing of Environment* **77** pp. 173–185.

STEFANOV, W. L. and NETZBAND, M., 2005, Assessment of ASTER land cover and MODIS NDVI data at multiple scales for ecological characterization of an arid urban center *Remote Sensing of Environment* **99** pp. 31-43.

STEFANOV, W. L. and NETZBAND, M., 2010, Characterization and monitoring of urban/peri-urban ecological function and landscape structure using satellite data *,* in RASHED, T. and JÜRGENS, C., eds., *Remote Sensing of Urban and Suburban Areas,* Springer, Dordrecht, pp. 219-244.

SU, W., ZHANG, C., YANG, J. Y., WU, H. G., CHEN, M. J., YUE, A. Z., ZHANG, Y. N., and SUN, C., 2010, Knowledge-Based Object Oriented Land Cover

Classification Using SPOT5 Imagery in Forest-Agriculture Ecotones *Sensor Letters* **8** pp. 22-31**.**

1. **Sutton, Paul C**.; Anderson, Sharolyn, J.; Elvidge, Christopher D.; Tuttle, Benjamin, T.; Ghosh, Tilottama (2009) *Paving the Planet*: *Impervious Surface as a Proxy Measure of the Human Ecological Footprint* Progress in Physical Geography 33(4) pp. 1-18

2. **Sutton, Paul C**.; Cova, Tom; Elvidge, Chris; (2006) *Mapping Exurbia in the conterminous United States using Nighttime Satellite Imagery* June 20(2) Geocarto International

U.S. CENSUS, 2010, http://www.census.gov/ (accessed 13 June 2010).

WELCH, R., 1980, Monitoring urban population and energy utilization patterns from satellite data *Environmental Management* **9** pp. 1-9.

WENG, Q., LU, D. and SCHUBRING, J., 2004, Estimation of land surface temperature-vegetation abundance relationship for urban heat island studies *Journal of Environmental Management* **70** pp. 145-156.

WENG, Q. and LU, D., 2008, A sub-pixel analysis of urbanization effect on land surface temperature and its interplay with impervious surface and vegetation coverage in Indianapolis, United States *International Journal of Applied Earth Observation and Geoinformation* **10** pp. 68-83.

WENTZ, E. A., STEFANOV, W., GRIES, L. and HOPE, D., 2006, Land use and land cover mapping from diverse data sources for an arid urban environments. *Computers Environment and Urban Systems* 30.3 (2006): 320-346.

WENTZ, E. A., NELSON, D., RAHMAN, A., STEFANOV, W. L. and SEN ROY, S., 2008, Expert system classification of urban land use/cover for Delhi, India *International Journal of Remote Sensing* **29** pp. 4405-4427**.**

Table 1: Overall accuracy scores using the four classification approaches

	ES	DA	DASW_F	DASW_A
Urban core	66.36%	16.36%	33.64%	31.82%
Residential	60.00%	19.09%	26.36%	29.09%
Urban fringe	58.18%	20.91%	21.82%	15.45%

Table 2: Producer and user accuracy scores for the three study areas for each classification approach

	Producer accuracy				User accuracy			
Class Name	ES	DA	DASW_F	DASW_A	ES	DA	DASW_F	DASW_A
Urban Core (a)								
Asphalt	58.33%	27.27%	27.27%	27.27%	70.00%	33.33%	42.86%	100.00%
Soil/bedrock	38.89%	15.38%	23.08%	23.08%	70.00%	9.09%	18.75%	13.64%
Agricultural Soil	100.00%	8.33%	25.00%	25.00%	60.00%	11.11%	37.50%	37.50%
Fluvial Sediments	87.50%	0.00%	0.00%	0.00%	70.00%	0.00%	0.00%	0.00%
Water	87.50%	25.00%	12.50%	12.50%	70.00%	25.00%	100.00%	100.00%
Agricultural Vegetation	80.00%	37.50%	50.00%	50.00%	80.00%	25.00%	33.33%	36.36%
Undifferentiated Vegetation	100.00%	---	---	---	80.00%	---	---	---
Grass/Shrubs	100.00%	0.00%	---	---	30.00%	0.00%	---	---
Mesic Residential	64.29%	0.00%	76.92%	69.23%	90.00%	0.00%	41.67%	40.91%
Xeric Residential	44.44%	43.75%	18.75%	18.75%	80.00%	46.67%	23.08%	21.43%
Reflective Built Surfaces	60.00%	0.00%	---	---	30.00%	0.00%	---	---
Residential (b)								
Asphalt	50.00%	0.00%	8.33%	8.33%	46.15%	0.00%	7.14%	7.14%
Soil/bedrock	68.18%	27.27%	18.18%	18.18%	35.71%	30.00%	30.77%	36.36%
Agricultural Soil	61.11%	44.44%	55.56%	50.00%	100.00%	42.11%	43.48%	34.62%
Fluvial Sediments	100.00%	0.00%	---	---	50.00%	0.00%	---	---
Water	---	0.00%	---	---	---	0.00%	---	---
Agricultural Vegetation	100.00%	28.57%	28.57%	42.86%	100.00%	13.33%	16.67%	20.00%
Undifferentiated Vegetation	0.00%	---	---	---	0.00%	---	---	---
Grass/Shrubs	100.00%	50.00%	0.00%	50.00%	66.67%	11.11%	0.00%	33.33%
Mesic Residential	22.22%	0.00%	0.00%	---	66.67%	0.00%	0.00%	---
Xeric Residential	58.06%	9.68%	35.48%	45.16%	81.82%	33.33%	29.73%	36.84%
Reflective Built Surfaces	66.67%	16.67%	16.67%	0.00%	66.67%	12.50%	12.50%	0.00%
Urban Fringe (c)								
Asphalt	50.00%	25.00%	0.00%	0.00%	22.22%	14.29%	0.00%	0.00%
Soil/bedrock	60.00%	40.00%	80.00%	73.33%	45.00%	30.00%	25.00%	19.30%
Agricultural Soil	60.00%	33.33%	---	---	90.00%	33.33%	---	---
Fluvial Sediments	100.00%	0.00%	---	---	37.50%	0.00%	---	---
Water	90.00%	30.00%	---	---	100.00%	60.00%	---	---
Agricultural Vegetation	50.00%	0.00%	0.00%	---	14.29%	0.00%	0.00%	---
Undifferentiated Vegetation	100.00%	---	---	---	75.00%	---	---	---
Grass/Shrubs	44.44%	0.00%	44.44%	33.33%	57.14%	0.00%	16.00%	9.68%
Mesic Residential	42.86%	9.52%	4.76%	---	75.00%	50.00%	25.00%	---
Xeric Residential	62.50%	18.75%	25.00%	6.25%	90.91%	17.65%	21.05%	8.33%
Reflective Built Surfaces	41.67%	25.00%	25.00%	16.67%	55.56%	33.33%	27.27%	25.00%

Table 3 Area in km^2 and percentage of total for the three study areas for each classification approach

	Area (km^2)				Percentage of Total			
Class	ES	DA	DASW_F	DASW_A	ES	DA	DASW_F	DASW_A
Urban Core (a)								
Asphalt	46.40	44.38	23.19	19.48	13.19%	12.61%	6.59%	5.53%
Soil/bedrock	133.12	47.17	65.41	70.11	37.83%	13.40%	18.59%	19.92%
Agricultural Soil	4.54	18.75	20.79	20.79	1.29%	5.33%	5.91%	5.91%
Fluvial Sediments	8.44	45.99	22.52	16.50	2.40%	13.07%	6.40%	4.69%
Water	1.77	28.47	2.61	2.13	0.50%	8.09%	0.74%	0.61%
Agricultural Vegetation	4.41	18.92	14.85	14.85	1.25%	5.38%	4.22%	4.22%
Undifferentiated Vegetation	2.22	2.04	2.14	0.77	0.63%	0.58%	0.61%	0.22%
Grass and Shrubs	13.64	27.36	0.12	0.12	3.88%	7.77%	0.03%	0.03%
Mesic Residential	28.58	22.52	139.40	140.46	8.12%	6.40%	39.61%	39.91%
Xeric Residential	84.13	46.84	60.42	66.70	23.91%	13.31%	17.17%	18.95%
Reflective Built Surfaces	24.66	49.47	0.46	0.00	7.01%	14.06%	0.13%	0.00%
Residential (b)								
Asphalt	34.27	29.36	38.10	36.50	9.75%	8.34%	10.83%	10.37%
Soil/bedrock	121.42	40.16	34.20	32.79	34.54%	11.41%	9.72%	9.32%
Agricultural Soil	27.43	66.55	68.57	72.43	7.80%	18.91%	19.49%	20.58%
Fluvial Sediments	5.61	44.41	2.36	1.32	1.60%	12.62%	0.67%	0.38%
Water	0.98	16.54	1.21	0.55	0.28%	4.70%	0.34%	0.16%
Agricultural Vegetation	24.12	41.14	44.68	47.10	6.86%	11.69%	12.70%	13.38%
Undifferentiated Vegetation	1.97	3.43	2.01	1.57	0.56%	0.97%	0.57%	0.45%
Grass and Shrubs	14.59	28.62	12.80	8.34	4.15%	8.13%	3.64%	2.37%
Mesic Buildings	27.21	18.20	8.11	3.57	7.74%	5.17%	2.30%	1.01%
Xeric Buildings	76.90	31.36	107.60	120.96	21.87%	8.91%	30.58%	34.37%
Reflective Built Surfaces	17.08	32.15	32.27	26.80	4.86%	9.14%	9.17%	7.62%
Urban Fringe (c)								
Asphalt	22.55	34.26	23.15	15.66	6.41%	9.74%	6.58%	4.45%
Soil/bedrock	182.34	65.28	204.53	236.05	51.81%	18.55%	58.12%	67.08%
Agricultural Soil	1.04	53.93	0.73	0.37	0.29%	15.33%	0.21%	0.11%
Fluvial Sediments	4.94	45.47	0.53	0.03	1.40%	12.92%	0.15%	0.01%
Water	0.60	19.22	0.36	0.03	0.17%	5.46%	0.10%	0.01%
Agricultural Vegetation	1.25	17.54	0.26	0.05	0.36%	4.98%	0.07%	0.01%
Undifferentiated Vegetation	1.55	1.10	0.18	0.01	0.44%	0.31%	0.05%	0.00%
Grass and Shrubs	11.81	23.67	39.52	36.90	3.36%	6.73%	11.23%	10.49%
Mesic Buildings	26.40	21.07	10.73	3.09	7.50%	5.99%	3.05%	0.88%
Xeric Buildings	84.04	40.58	43.35	39.74	23.88%	11.53%	12.32%	11.29%
Reflective Built Surfaces	15.40	29.80	28.58	19.98	4.38%	8.47%	8.12%	5.68%

Figure Captions

Figure 1: The Phoenix metropolitan area shown in false colour with the location of the three study areas indicated

Figure 2: The urban core study area classified with a) expert system; b) discriminant analysis; c) discriminant analysis with spatial weights using a fixed bandwidth; and d) discriminant analysis with spatial weights using an adaptive bandwidth

Figure 3: The residential study area classified with a) expert system; b) discriminant analysis; c) discriminant analysis with spatial weights using a fixed bandwidth; and d) discriminant analysis with spatial weights using an adaptive bandwidth

Figure 4: The urban fringe study area classified with a) expert system; b) discriminant analysis; c) discriminant analysis with spatial weights using a fixed bandwidth; and d) discriminant analysis with spatial weights using an adaptive bandwidth

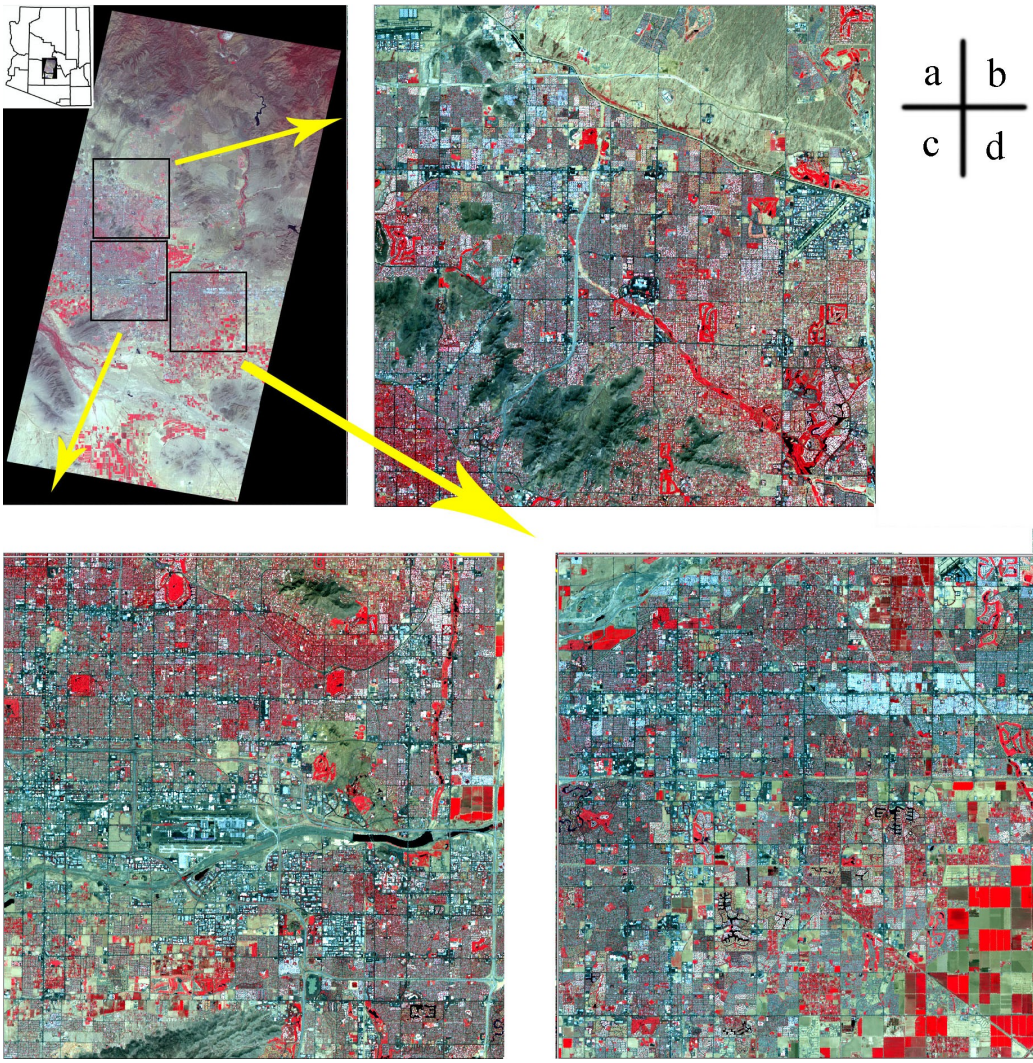

Figure 1

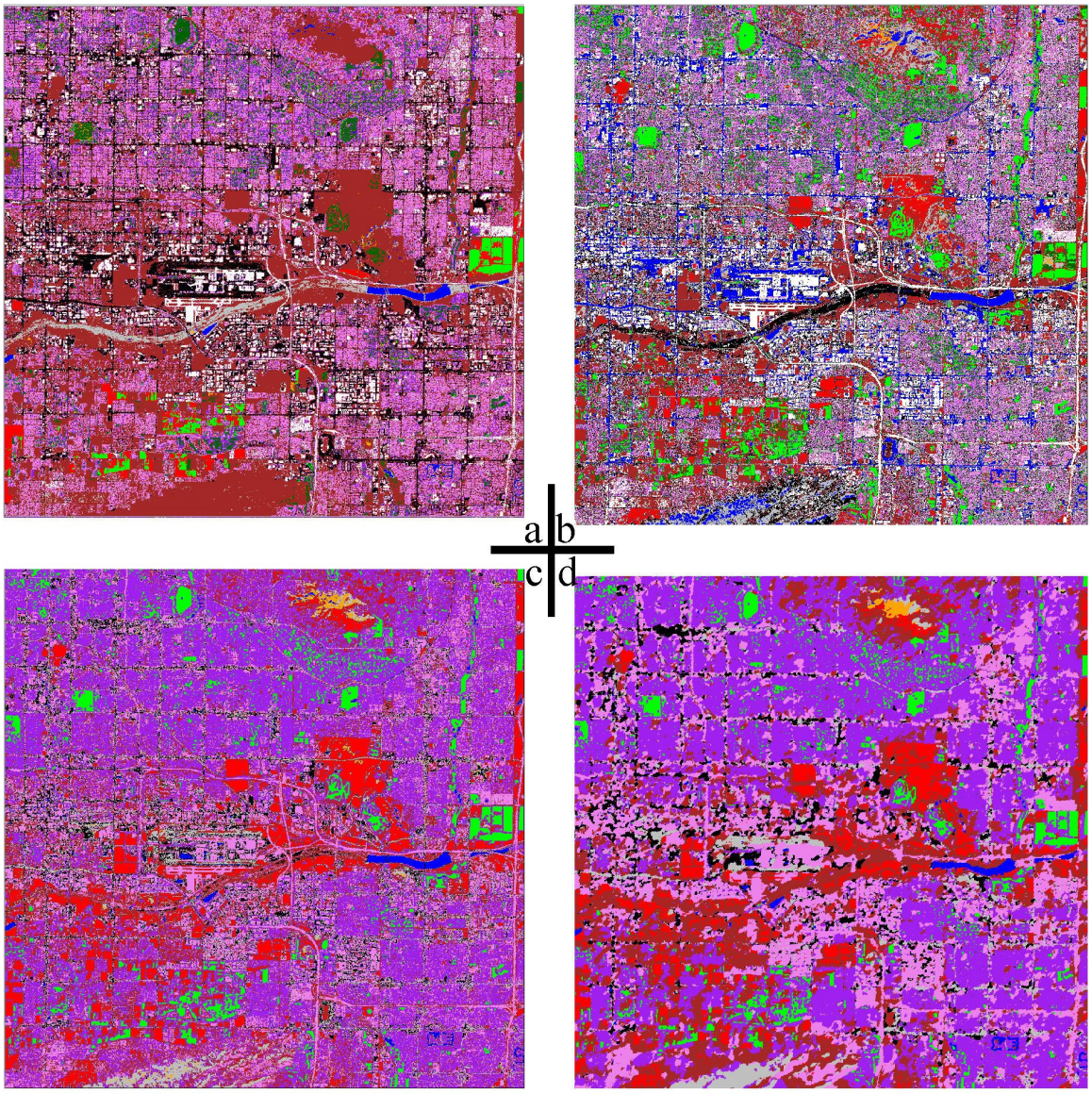

Asphalt		Fluvial Sediments	
Soil/Bedrock		Water	
Agriculttural Soil		Agricultural Vegetation	
Grass and Shrubs		Undifferentiated Veg	
Mesic Built		Xeric Built	
		Reflective Surface	

Figure 2

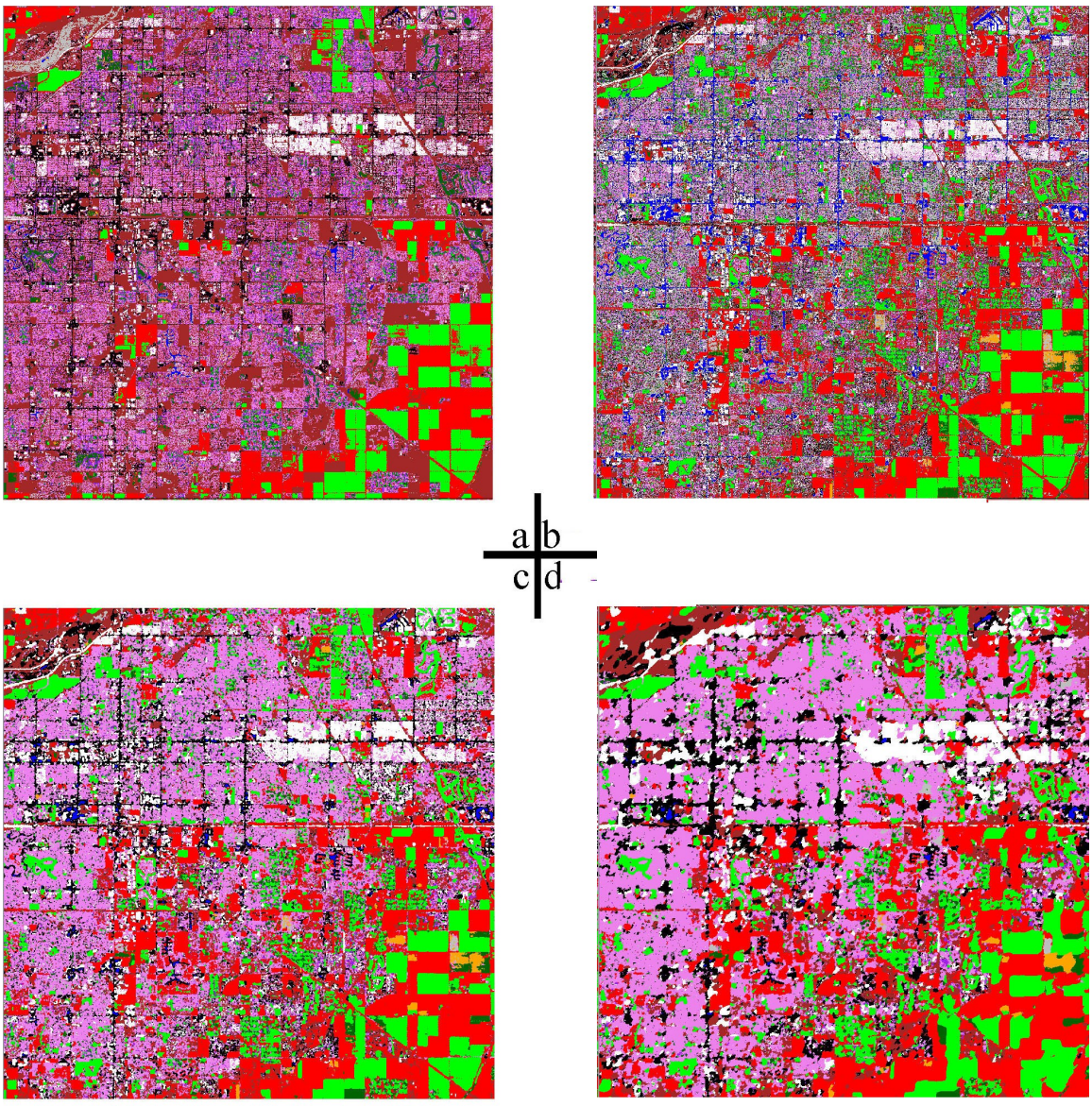

Asphalt		Fluvial Sediments	
Soil/Bedrock		Water	
Agricultttural Soil		Agricultural Vegetation	
Grass and Shrubs		Undifferentiated Veg	
Mesic Built		Xeric Built	
		Reflective Surface	

Figure 3

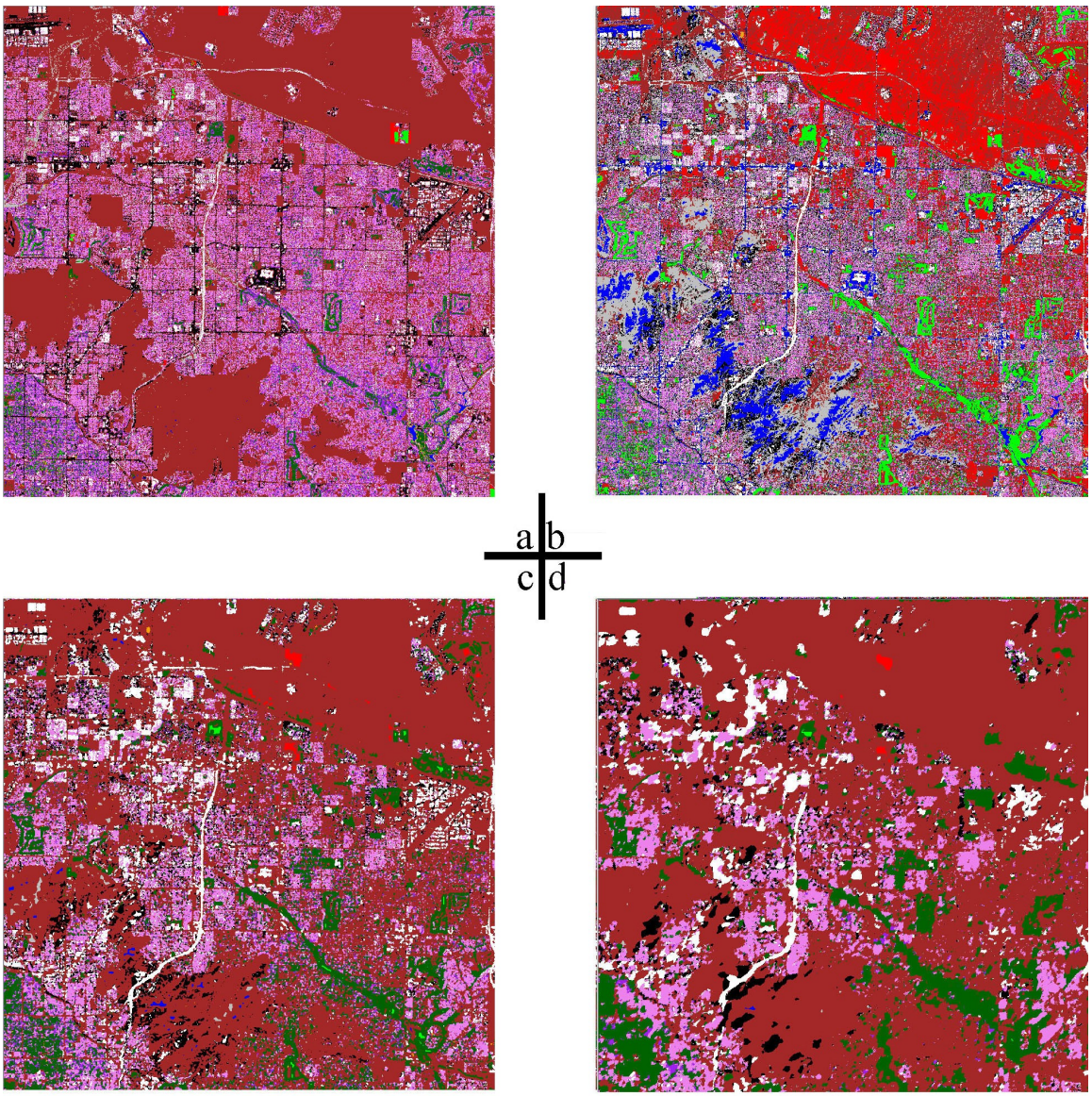

Asphalt		Fluvial Sediments	
Soil/Bedrock		Water	
Agriculttural Soil		Agricultural Vegetation	
Grass and Shrubs		Undifferentiated Veg	
Mesic Built		Xeric Built	
		Reflective Surface	

Figure 4